ELSEVIER

Polymer 42 (2001) 4579–4587

polymer

www.elsevier.nl/locate/polymer

Crystallisation of single-site polyethylene blends investigated by thermal fractionation techniques

F. Chen, R.A. Shanks*, G. Amarasinghe

[a]*Department of Applied Chemistry, RMIT University, G.P.O. Box 2476V, Melbourne, Vic. 3001, Australia*

Received 27 September 2000; received in revised form 1 November 2000; accepted 29 November 2000

Abstract

Branched polyethylenes, low density polyethylenes (LDPE) or long-chain branched very low density polyethylenes (VLDPE), were blended with VLDPEs containing short branches. The melting behaviour of pure copolymers and their blends were investigated using differential scanning calorimetry (DSC) after applying stepwise isothermal crystallisation ('thermal fractionation'). Thermal fractionation separates polymers according to their branching densities and fractionated curves used to determine the short-chain branching distribution (SCB), crystallisation and miscibility of blends. When both polymers have similar unbranched segments, they may co-crystallise if they are miscible in the melt. The co-crystallisation is observed to occur in all sets of blends, however, the extent of co-crystallisation varies from blend to blend. The blends of metallocene-catalysed VLDPE1 and LDPEs show significant deviation from the additivity rule indicating the greater co-crystallisation and hence melt miscibility at all compositions. The extent of co-crystallisation decreases for the VLDPE1 blends containing long-chain branched VLDPE2 and increases for Ziegler–Natta-catalysed VLDPE3–VLDPE2 blends, as the VLDPE2 content increases. DSC fractionated curves allow detailed examination of co-crystallisation and miscibility of blends that is also comparable to the results gained by temperature rising elution fractionation.

Keywords: Crystallisation; Single-site polymers; Polyethylene blends

1. Introduction

The characterisation of polymer blends by new and improved analytical techniques is of great interest. Temperature rising elution fractionation (TREF), a technique that fractionates polymers according to the crystallisability is the frequently used method to analyse molecular heterogeneity parameters of polymers [1]. Due to the lengthy steps, handling of large amount of toxic solvents and high cost involved TREF procedures are not amenable to use in most laboratories. Nevertheless, the TREF separation becomes less effective as the crystallinity of polymer is decreased. Therefore, alternative methods [2,3] including fractionation methods in a differential scanning calorimetry (DSC) have been considered. Many of these DSC fractionation methods are based on the subsequent analysis of melting behaviour of the sample after applying a particular thermal treatment such as stepwise annealing [4,5], stepwise cooling [5–18] and combination of the above procedures [5,19].

Our group has recently investigated a stepwise slow cooling program (called 'thermal fractionation') to fractionate different grades of ethylene copolymers [20–22] and blends [23,24]. During the crystallisation, molecules or segments of molecules containing similar branch densities are separated and crystallised together. Also, the short branches and the branch points of long branches are excluded from the crystals; however, the long branches participate in crystallisation. It is generally believed that branches which are longer than methyl or ethyl are mostly excluded from the crystal lattice [25]. The extent of incorporation of branches within the crystal are mainly dependent on the crystallisation conditions, and rapid or quenched crystallisation allows certain branched types to be included in the crystals [26]. Moreover, it has been shown that it is the branch content rather than branch type that is important in determining crystallisation [27]. However, the exclusion of branch points from crystals should be completed due to the long equilibration time used (50 min) at each isothermal crystallisation temperature. Consequently, after thermal fractionation, the polymer crystal contains a group of lamellae of different thickness, which are separated according to the branching densities. Liu and co-workers [28] have recently shown that the ethyl and hexyl branches are in fact excluded from the crystal, and a considerable amount of crystal perfection is observed to occur in single-site polymers during the thermal fractionation process. The thermal fractionation

* Corresponding author. Tel./fax: +61-3-9925-2122.
E-mail address: robert.shanks@rmit.edu.au (R.A. Shanks).

0032-3861/01/$ - see front matter
PII: S0032-3861(00)00859-4

principle is similar to TREF, however, no actual physical separation is obtained.

The applications of DSC fractionation to polymers include analysis of short-chain branching distribution (SCB), phase separation [12,14], miscibility behaviour of blends [23,24,29] and reaction mechanism for grafting [13,30,31], etc. Most of the emphasis is on the characterisation of copolymers by analysing the ethylene run sequence between branch points [6,11,13,15,17,18,20,22–24,29,31]. Recently, Müller and co-workers [29] have applied successive self-nucleation/annealing (SSA) [19] method, which is based on the superposition of self-nucleation and annealing cycles, to evaluate the miscibility of high density polyethylene (HDPE)–linear low density polyethylene (LLDPE) blends. We have also used a stepwise slow cooling program to examine the co-crystallisation and miscibility of octene LLDPE–very low density polyethylene (VLDPE) [23] and hexene rich LLDPE–low density polyethylene (LDPE) blends [24]. When used in conjunction with other analytical techniques, DSC fractionation has also been useful in elucidating the components of unidentified blends[11,16,31,32].

LLDPEs are often blended with LDPEs in order to improve the processability and optical properties [33]. The morphology of these blends is determined by the phase segregation and/or miscibility of polymers in the blend which is strongly dependent on the branch concentration, blend composition and crystallisation conditions. Numerous studies have been devoted to investigate the crystallisation behaviour of LLDPE–LDPE blends, however, the phenomena of co-crystallisation and separate crystallisation is still controversial. Since most of these works are performed on blends of Ziegler–Natta (ZN)-catalysed LLDPE that contain considerable compositional heterogeneity, it is difficult to distinguish which portion of the molecule takes part in the co-crystallisation or separate crystallisation. Nonetheless, single-site catalyst technology allows synthesising of polymers with comparatively narrower molecular weight distributions along with almost uniformly distributed narrower branch distributions. Because of their well-defined molecular structures, the blends containing single-site polymers are expected to alleviate the problems occurring in the blends of ZN-catalysed LLDPEs. The frequently studied blends are those in which one component is HDPE [34–38]. Zhao et al. [36] and Lee and Jho [38] concluded that the ZN LLDPEs are more miscible to HDPE than metallocene LLDPEs. It is argued that the heterogeneity of the molecular and composition distributions of ZN LLDPE causes easier co-crystallisation whereas, more uniform distribution makes it difficult. Furthermore, the studies on these blends have shown that as the branch content of the single-site polymer is increased, co-crystallisation diminishes and results in the formation of two phases [34,35,37].

In this study, the crystallisation and miscibility behaviour of single-site polyethylene blends were investigated after subjecting them to a sequential slow crystallisation program in a DSC. The variation in crystal population under each lamella with an addition of the second polymer was particularly examined. In addition, the distribution of SCB of pure copolymers and blends are also evaluated. These blend systems are especially designed to introduce long branches into a polymer that has only short branches, expecting to modify the morphology of blends so that the properties such as haze, gloss and strain hardening are improved.

2. Experimental

The polymers used in this study are commercial polyethylenes and the characteristics of these polymers are presented in Table 1. 1-Butene, 1-octene copolymers and LDPEs were supplied by Kemcor Australia Ltd., Dow Plastics, and Orica Pty Ltd., respectively. These polymers were selected because they contain overlapping regions of melting or molecules with common unbranched segments. The LLDPEs of densities between 0.89 and 0.91 g cm^{-1} are called VLDPEs [39] and the following four blend sets were prepared.

1. VLDPE1–LDPE1
2. VLDPE1–LDPE2
3. VLDPE1–VLDPE2
4. VLDPE3–VLDPE2

In these systems, all the first components, VLDPE1 and VLDPE3 contain only short-chain branches, whereas all the second components, LDPE1, LDPE2 and VLDPE2 have both short and long-chain branches.

2.1. Blend preparation

The blends with varying compositions (by weight) were prepared by melt extrusion using an Axon BX-12 single-screw extruder (Axon Australia Pty. Ltd.) with a Gateway screw of 12.5 mm diameter and a length:diameter ratio of 26:1. The operating temperature profile was 140, 195, 200 and 170°C, for feeding, compression, metering and die-end zone, respectively and the screw speed was 60 rpm. The hot strands of the blends were quenched in water at room temperature, dried and finally granulated.

2.2. Differential scanning calorimetry

The DSC measurements were performed on a Perkin–Elmer Series DSC7 calorimeter under a nitrogen purge (15 ml min^{-1}). Sample masses of 3–4 mg were encapsulated in aluminium pans with a crimper and the samples were first melted at 180°C for 5 min to remove previous thermal history. The samples were then cooled to 10°C at a rate of 10°C min^{-1} and reheated to 180°C at the same rate. The melting (T_m) and crystallisation (T_c) temperatures were measured. The baseline scan was performed using a similar

Table 1
Properties of polymers

Properties	VLDPE1[a]	VLDPE2[b]	VLDPE3[c]	LDPE1[d]	LDPE2[d]
Comonomer	Butene	Octene	Octene		
Catalyst type[e]	M	S	ZN	P	P
MFI (dg min^{-1})	27.0	1.0	1.0	7.0	22.0
Density (g cm^{-3})	0.901	0.908	0.912	0.919	0.918
M_w	58,000	96,700	1,20,000	4,74,000	89,000
M_w/M_n	2.65	2.86	3.80	23.3	4.4
Comonomer content (mol%)	6.3	2.4	4.2		
T_m (°C)	92.7	105.4	123.0	106.5	103.9
T_c (°C)	76.6	90.3	100.5	87.8	87.1

[a] Ref. [34].
[b] Ref. [35].
[c] Refs. [28,48].
[d] Data were taken from chemical data sheets published by the manufacturer.
[e] ZN: ZN catalyst; S: Constrained geometry single-site catalyst; M: Metallocene; and P: Peroxide.

empty pan. The calorimeter was calibrated for temperature and heat flow using indium and zinc standards and the calibration was regularly checked against the onset melting temperature of indium.

2.3. Thermal fractionation method

Thermal fractionation was carried out in a Perkin–Elmer Pyris1 DSC flushed with dry nitrogen. Before the fractionation, all the samples were held at 180°C for 5 min to eliminate any effects from previous thermal memory. The samples were then rapidly cooled to the first isothermal crystallisation temperature (T_{c1}) at a rate of 200°C min^{-1} and held for 50 min. Subsequently, the samples were again cooled to the next T_{c2} at a rate of 200°C min^{-1} and the isothermal crystallisation was followed for another 50 min. Then the process was repeated at intervals of 4°C until the final temperature reached 24°C. The average cooling rate used here was 0.08°C min^{-1}, which was in the order of the rate used in TREF analysis.

Different temperature ranges were selected for different types of polymers and their blends. The T_{c1} for VLDPE3 and the blends of VLDPE3–VLDPE2 was 124°C, whereas 116°C was used as the T_{c1} for all other polymers and blends. The T_{c1} values were calculated by adding 12°C (three 4°C steps) to the crystallisation onset temperature at 0.08°C min^{-1} rate ($T_{c,0.08}$), which was obtained from the cooling rate versus crystallisation onset temperature curves. Finally, their melting behaviour was obtained by heating the treated samples from 10 to 150°C at a rate of 10°C min^{-1} on a Perkin–Elmer DSC7.

2.4. Data analysis

The specific heat curve was calculated from raw heat flow curve by using Pyris software version 3.72. The relationships between melting peak temperature (T_{mx}, where $x = 1, 2, 3, \ldots$), short-chain branching (B) and degree of crystallinity (χ_c), which were derived from TREF data reported by Hosoda [40], were as follows [22].

1-butene comonomers $T_{mx} = -1.55B + 134$

$\chi_c = -1.32B + 82,$

1-octene comonomers $T_{mx} = -2.18B + 134$

$\chi_c = -2.51B + 86.$

Furthermore, the amount of polymer under each fraction was estimated using the following equation, %Polymer = (partial area/%χ_c) × 100.

3. Results and discussion

3.1. Optimum conditions for thermal fractionation

The thermal fractionation technique used here is a stepwise slow cooling program. In order to achieve a better fractionation for individual polymers, careful selection of experimental parameters, such as T_{c1}, temperature interval, isothermal time and the final isothermal crystallisation temperature (T_{cf}) is very important. The T_c values of pure polymers are within the range of 75–101°C at a rate of 10°C min^{-1} (Table 1). Since the thermal fractionation is carried out at an average rate of 0.08°C min^{-1}, it is necessary to obtain $T_{c,0.08}$ values for each polymer. These values are estimated by plotting the cooling rate versus $T_{c,onset}$ curves. The determination of T_{c1} is very important because the isothermal crystallisation is very sensitive to the temperature chosen. If the sample was directly cooled to $T_{c,0.08}$ from the melt at a fast cooling rate of 200°C min^{-1}, the actual temperature of the sample would shoot to about 0.5–0.6°C below the program temperature ($T_{c,0.08}$) in the DSC. Under this circumstance, the sample becomes

overcooled and the crystallisation can be initiated producing incorrect thermal fractionation data. Accordingly, it is necessary to select a higher temperature that keeps the sample completely in the melt as the first isothermal crystallisation temperature, and the T_{c1} is then determined by adding three 4°C consecutive isothermal crystallisation steps (total of 12°C) to the $T_{c,0.08}$ values.

In order to examine the sensitivity of T_{c1} to the fractionation, VLDPE2 was fractionated at various temperature ranges (115–23, 116–24, 117–25 and 118–26°C) and the melting curves obtained after fractionation are shown in Fig. 1. The curves reveal the importance of the starting crystallisation temperature. When the T_{c1} increased from 115 to 118°C, the large double peaks showed a progressive change in the ratio of the two peaks, from two approximate peaks to one peak with a small shoulder. At the same time, the peak temperatures of the double peak were also increased from 107, 108, 109 to 110°C (a shoulder) for T_{m1} and from 103, 104, 105 to 106°C for T_{m2}. This suggests that the temperature of 118°C was too high a temperature for most of the lightly branched molecules to crystallise. As the starting crystallisation temperature was decreased by 1°C each time, more lightly branched fractions could crystallise. The next highest melting peak (T_{m3}) exhibits a similar change in area (crystal population) with the largest peak appearing at the highest T_{c1}. The rest of the melting peaks were approximately constant in the area for each fractionation. The maximum resolution between peaks was achieved with temperature intervals of 4°C. If less than 4°C was used, the peaks were likely to merge [41].

Two isothermal crystallisation times of 50 and 100 min were tested for long-branched VLDPE2 and LDPE2 polymers. The same resolutions were obtained for each polymer at each isothermal time suggesting that stepwise cooling program used here with 50 min holding time will allow adequate time to form crystals. Therefore, the 50 min holding time was selected for the experiments. Moreover, in order to determine a suitable T_{cf}, the polymers were fractionated within the ranges of 116–24 and 116–44°C. It was found that only the fractionated curves of VLDPE1 were different under the various T_{cf}. In the curve obtained with a higher T_{cf} (44°C), the region especially below 44°C did not show any fractionation while better fractionation was seen with T_{cf} of 24°C. Such a relatively low melting range (24–105°C) of VLDPE1 (see the bottom curve in Fig. 2) is due to the wide SCB of this polymer.

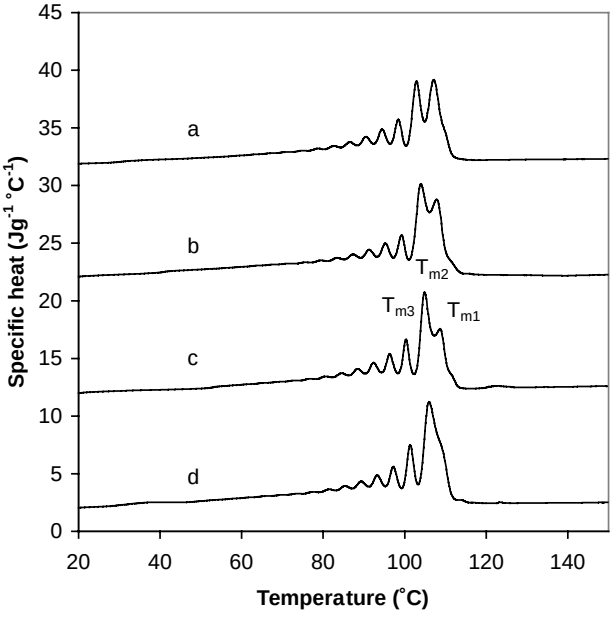

Fig. 1. DSC specific heat melting curves of VLDPE2 after thermal fractionation at different temperature ranges: (a) 115–23; (b) 116–24; (c) 117–25; and (d) 118–26°C. An adapted scale is drawn by consecutively adding 10 units to each curve.

3.2. LDPE blends

Fig. 2 displays the melting curves of VLDPE1–LDPE1 blends after thermal fractionation. All curves show a series of melting peaks that depict the melting of crystallites of specific branch density. The number of peaks in the melting curves correspond to the number of crystallisation steps used in the thermal fractionation program below the onset of crystallisation temperature of the polymer. Also, the peak melting temperatures for all polymers are almost the same since they are determined by the stepwise isothermal temperatures used in thermal fractionation. LDPE1 (top curve) shows a large unresolved double peak preceded by a series of small lower temperature peaks in the range of 60–108°C. These characteristic peaks are preserved and the double peak gets more resolved in the blends as the LDPE1 is diluted by VLDPE1. VLDPE1 also contains a series of peaks covering the range 50–105°C with the peak at 92°C being the largest. As we can see from the figure, a new set of peaks develop at around 111°C when LDPE1 composition decreases. This is unexpected because VLDPE1 does not show any melting peaks above 98°C and the LDPE1 shows melting peaks only below 108°C. The presence of such an additional endotherm has also been observed for slowly-cooled LLDPE–LDPE blends by other researchers [24,42].

Two explanations can be envisaged for the growth of the new peak. It may suggest the development of a miscible phase that arises from the co-crystallisation between the molecules, with the longest segments between branches from the VLDPE1 and LDPE1 or it can be considered as a consequence of nucleation of VLDPE1 by LDPE1. The formation of a miscible co-crystalline phase has also been detected between the linear or lightly branched portions of HDPE and LDPE in HDPE–LDPE blends and is confirmed by preparative TREF by Fonseca and Harrison [43]. The nucleating effect of LLDPE has been observed when the temperature is held above the melting of pure branched polyethylenes (LDPE) [44,45]. Here, since VLDPE1 remains as liquid above 105°C, LDPE1 phase can act as a

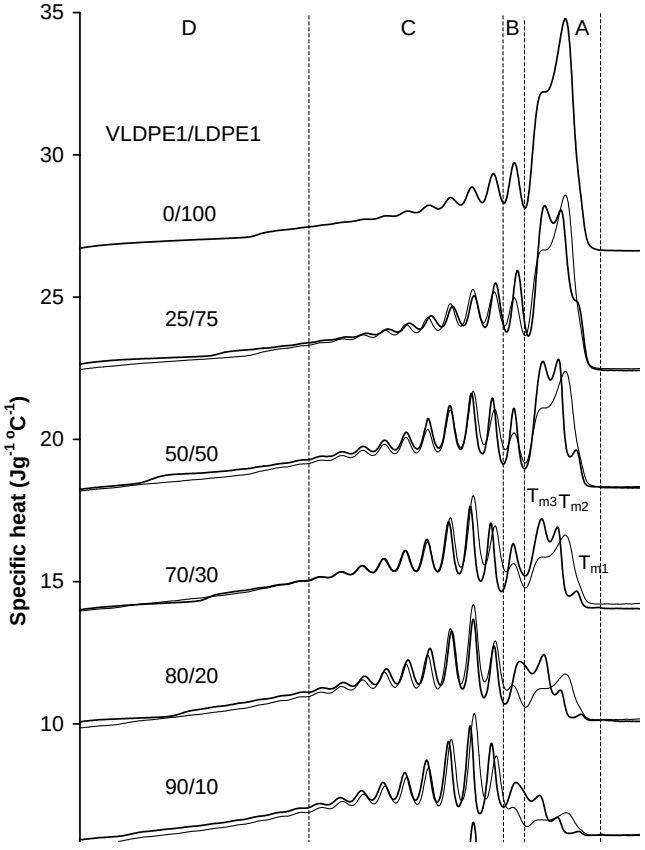

Fig. 2. DSC specific heat melting curves for blends of VLDPE1–LDPE1 and the pure polymers after thermal fractionation. Thin solid lines represent the calculated specific curves for the blends. An adapted scale is drawn by consecutively adding 4 units to each curve. First number of the ratio indicates the amount of VLDPE1.

nucleating agent of VLDPE1 phase, allowing little co-crystallisation to occur.

The influence of blending was further examined by comparison with calculated curves (thin solid lines) which were obtained by adding the component specific heat curves in the same proportion in which they were present in the blend. The DSC curves of each polymer will be an additive in the blend if blends crystallise in the same way as in the pure polymers. The peaks in the lower temperature melting regions ($T_m < 97$°C) are additive as shown by the coincidence of the calculated and experimental melting curves, however, the higher melting peaks are not clearly additive. A greater disagreement is seen for the lightly branched or linear part of the molecule. The calculated curve displays a unresolved main melting peak for LDPE1, whereas the observed curve contains two resolved peaks within the same temperature range. Furthermore, the newly developed peak (T_{m1}) is also not observed in the calculated curve. The ratios of partial area between experimental and calculated curves obtained in the four temperature regions are shown in Table 2. Since the crystal population is proportional to the area under each peak, the ratios greater than one indicate an increase in population and vice versa. The significant deviation from one is clearly seen for the entire compositions. Interestingly, the remarkable changes are observed for blends containing up to 30% LDPE. The increase in population in regions A–B and decrease in C–D clearly indicates the shift of the population to higher temperatures. These differences suggest that the two polymers are having an effect on their crystallisation in the blend. Therefore, they are able to co-crystallise at all compositions and could be miscible or partially miscible in the melt. The miscibility of blends has also been examined by preparative TREF [43,46], and the TREF analysis on mixtures of LLDPE and LDPE suggests that fractions containing similar branches are more likely to miscible than fractions with different branch contents, indicating co-crystallisation between the similar branch segments [46]. Moreover, the use of specific heat curves for the DSC results has enabled this procedure to be used since heat flow curves only provide relative DSC curves.

Similar trends of melting are seen for the fractionated blends of VLDPE1–LDPE2 and the pure LDPE2 (not shown here). The main difference between LDPE1 and LDPE2 is the polydispersity (i.e. melt flow index) of the polymers, and therefore, the melting behaviour of these two blends indicates that the polydispersity or molar mass has no effect on co-crystallisation as suggested by other researchers [47]. This is not surprising since it is the unbranched segments that co-crystallise not the whole molecule under the thermal fractionation. If the fractionation were influenced by mutual solubility of polymers in the blend, then differences would be expected. Molar mass does influence solubility, so in these blends it is likely that the two polyethylenes are completely soluble.

3.3. VLDPE1–VLDPE2 blends

VLDPE1 and VLDPE2 are both single-site-initiated copolymers. VLDPE1 is a traditional metallocene-catalysed ethylene–butene copolymer containing only short branches whereas VLDPE2 is an ethylene–octene copolymer with incorporated long-chain branches, which is produced by the Dow constrained geometry catalyst technology (CGCT) [48,49]. The specific heat melting curves of blends of VLDPE1–VLDPE2 after thermal fractionation are shown in Fig. 3, and the corresponding partial area ratios are given in Table 2. Again, the appearance of a small peak (T_{m1}), above 110°C is seen suggesting that some molecular segments within butene VLDPE1 must be long enough to crystallise into octene VLDPE2 lamellae at higher temperatures. The fractions melting below 97°C show close agreement between the calculated and experimental curves, whereas the melting region above 97°C where only the VLDPE2 melts displays significant changes. As seen from Table 2, the partial area ratios have changed with the composition of VLDPE1, however, the changes with lightly branched molecules (regions A and B) are rather significant when VLDPE2 content is below 50%. These changes reveal

Table 2
Partial area ratios between the experimental and calculated curves of blends

	Partial $area_{exp}$/partial $area_{cal}$			
	A (>101°C)	B (97–101°C)	C (62–97°C)	D (<62°C)
VLDPE1–LDPE1				
75% LDPE1	1.05	1.32	0.94	0.94
50% LDPE1	1.12	1.16	0.97	0.89
30% LDPE1	1.41	1.67	0.89	0.93
20% LDPE1	1.23	2.42	0.91	0.97
10% LDPE1	1.37	2.70	0.91	0.98
VLDPE1–LDPE2				
75% LDPE2	1.15	1.05	0.94	0.93
50% LDPE2	1.28	1.36	0.89	0.98
30% LDPE2	1.30	2.21	0.88	0.96
20% LDPE2	0.84	2.36	0.93	1.01
10% LDPE2	1.45	2.01	0.92	1.03
VLDPE1–VLDPE2				
75% VLDPE2	1.06	1.26	0.92	1.04
50% VLDPE2	1.35	1.31	0.85	0.99
30% VLDPE2	1.51	1.63	0.88	0.93
20% VLDPE2	1.37	1.61	0.91	1.05
10% VLDPE2	1.23	1.92	0.94	1.02
	A (>113°C)	B (101–113°C)	C (73–101°C)	D (<73°C)
VLDPE3–VLDPE2				
75% VLDPE2	1.13	0.94	1.13	0.77
50% VLDPE2	1.10	0.91	1.08	0.90
30% VLDPE2	0.96	0.94	1.07	1.02
20% VLDPE2	0.98	0.91	1.05	1.11
10% VLDPE2	0.93	0.95	1.03	1.20

that there is some co-crystallisation and hence partial miscibility at these compositions. However, the extent of co-crystallisation apparently decreases at VLDPE2 content of 50% or more. Similar behaviour was also found for HDPE–VLDPE2 blends, cooled at a rate of 10°C min^{-1}, by Schellenberg and Wagner [35]. In this study, they also found that polymers were not miscible over entire composition range and phase separation occurred at above 50% or higher VLDPE2 contents. While, Hill and Barham have constructed the morphology maps for the blends of VLDPE1, they observed the single morphologies for all compositions for the rapidly quenched blends of butene VLDPE1–hexene VLDPE with similar branch contents (6.3 mol%) while, two crystal types were seen when the branch content is varied [50]. Thus, these mixed blends (ethylene–butene and ethylene–octene) with different average branch contents (6.3 versus 2.4 mol%) show some phase separation and/or miscibility as the VLDPE2 composition is varied.

It is proposed that these co-crystallisation and changes to the crystallinity in blends are responsible for the modification of the mechanical and optical properties of films, such as increased gloss and reduced haze. Nonetheless, the long branches of VLDPE2 are not drastically influenced by these properties, yet they are expected to increase the shear thinning characteristics of the rheology due to the reduced amount of long-chain branches at 0.01–1 per 1000 carbons [49].

3.4. VLDPE3–VLDPE2 blends

Fig. 4 illustrates the DSC specific heat melting curve for the thermally fractionated blends of VLDPE3–VLDPE2. VLDPE3 is a ZN-initiated ethylene–octene copolymer, which reflects a broader distribution of short-chain branches compared to those of single-site initiated VLDPE1 and VLDPE2. The calculated and observed curves were closely matched in the blends below 20% VLDPE2 blend indicating that two polymers could have crystallised independently. In contrast, above 30% VLDPE2 blend displayed significant differences between the calculated and observed curves. The most prominent difference is the better resolution at 107 and 103°C peaks in the experimental curves and the resolution between the calculated and experimental curves is improved as the VLDPE2 content decreases. The partial area ratios, shown in Table 2, are approximately constant when the content of VLDPE2 reduces, indicating that co-crystallisation diminishes as long-chain branched octene VLDPE2 content decreases. Again, in these blends where the branch

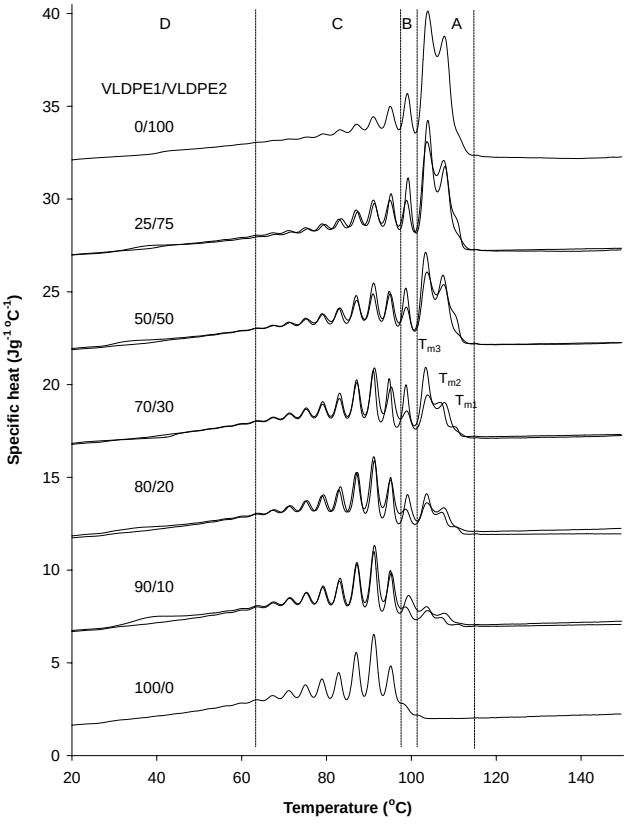

Fig. 3. DSC specific heat melting curves for blends of VLDPE1–VLDPE2 and the pure polymers after thermal fractionation. Thin solid lines represent the calculated specific curves for the blends. An adapted scale is drawn by consecutively adding 5 units to each curve. First number of the ratio indicates the amount of VLDPE1.

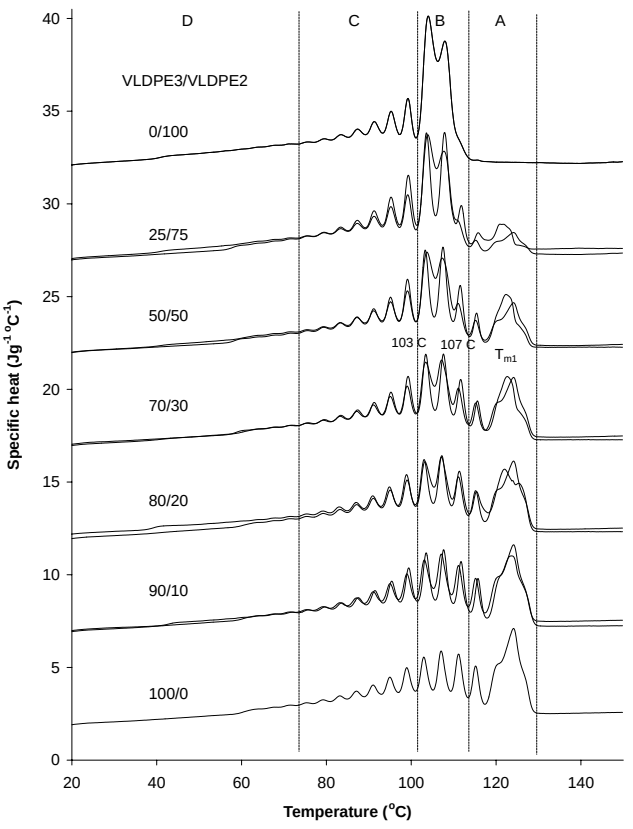

Fig. 4. DSC specific heat melting curves for blends of VLDPE3–VLDPE2 and the pure polymers after thermal fractionation. Thin solid lines represent the calculated specific curves for the blends. An adapted scale is drawn by consecutively adding 5 units to each curve. First number of the ratio indicates the amount of VLDPE3.

content is dissimilar (2.4 versus 4.2 mol%), co-crystallisation/separate crystallisation is seen.

Compared with the results from standard DSC curves obtained after cooling at 10°C min^{-1} for same blends, similar conclusions for the morphology of the blends are obtained [51], but thermal fractionation is a more sensitive method and provides more details. In addition, thermal fractionation is also useful in situations where the copolymers exhibit broad melting peaks over a wide range making DSC data less clear.

3.5. Short-chain branch distribution of the blends and pure polymers

As mentioned earlier, during the thermal fractionation, the branches are excluded from the crystal and the segment length of ethylene unit will limit the lamella thickness. Therefore, subsequent melting of fractionated polymer can reveal the lamella thickness distribution and hence SCB distribution. Since Hosoda [40] has first suggested the compositional distribution analysis from DSC data for LLDPEs, many researchers [7,15,17,22,23,29,31] have correlated melting temperature obtained using DSC with the degree of branching obtained by TREF analysis. A linear relationship between T_m and SCB is assumed, and the relationship depends on the type of comonomer. The SCB distributions of VLDPE2 and VLDPE3, calculated using the above equations are given in Table 3. It can be seen that the distributions of short-chain branches for the three types of polymers are quite different and not very homogeneous. ZN-type VLDPE3 has very broad SCB distribution (from 5 to 29), and these values are also in agreement with results obtained for LLDPE (0–30) by TREF analysis. In contrast, VLDPE1 and VLDPE2 have relatively narrow SCB distribution, but their ranges are different, that is, from 12 to 27 for VLDPE2 and from 25 to 45 for VLDPE1. This is to be expected due to the single-site nature of the catalysts used for the polymerisation of VLDPE1 and VLDPE2. If every component in the blend has the same comonomer and the type of comonomer is known, the SCB distribution for the blends can be obtained. Calculated branch densities along with SCB distribution for the blends of VLDPE3–VLDPE2 are presented in Table 3, which shows different branch densities with different composition ratios of the blends. The melting peaks within the fractionated DSC curves are a function of the fractionation

Table 3
Short-chain branching distribution versus amount of polymer in each fraction for copolymers and ethylene–octene VLDPE3–VLDPE2 blends

T_{mx} (°C)	Branches/ 1000 C	100% VLDPE2	75% VLDPE2	50% VLDPE2	30% VLDPE2	20% VLDPE2	10% VLDPE2	100% VLDPE3
125	4					3.7		
122	5		4.3	8.9	11.0	9.0	14.3	16.7
116	8		1.8	2.3	2.9	4.1	3.5	4.1
112	10		3.7	5.0	5.2	5.8	5.6	6.2
108	12	17.7	14.0	10.2	8.9	8.2	8.0	7.5
103	14	22.1	14.4	10.7	9.8	8.5	8.4	7.7
99	16	8.1	10.2	8.5	8.4	7.6	7.7	7.2
95	18	8.5	9.5	7.9	7.6	7.5	7.3	7.0
91	20	8.7	8.7	7.5	7.1	7.1	7.3	6.8
87	21	8.3	8.3	7.3	7.2	7.0	6.7	6.8
83	23	8.3	8.1	7.5	7.4	7.2	6.9	6.4
80	25	9.0	8.4	7.4	7.3	7.3	7.1	6.9
76	27	9.4	8.5	8.1	7.6	7.6	7.8	7.8
72	29			8.7	9.7	9.4	9.3	9.0

conditions, but they do reflect the distribution of branches within each polymer.

4. Conclusions

The thermal analysis of the blends of VLDPE1 or VLDPE3 with short-chain branches and LDPEs or VLDPE2 with long-chain branches after thermal fractionation has shown that the co-crystallisation occurs between the two polyethylenes in most blends according to the deviation from the additivity rule. It is also found that the level of co-crystallisation is different for each blend set. For the blends of VLDPE1–LDPEs, the co-crystallisation is found to occur at all compositions, and the presence of similar morphologies between the blends of VLDPE1–LDPE1 and VLDPE1–LDPE2 also indicates that molar mass or polydispersity is not important. However, the co-crystallisation for the blends of VLDPE1 and long-chain branched VLDPE2 increases with decreasing VLDPE2 content, while the co-crystallisation for the ZN-catalysed VLDPE3–VLDPE2 blends decreases with decreasing VLDPE2 content. Nevertheless, VLDPE2 did not cause a significant change in the morphology of VLDPE1 and VLDPE3, perhaps due to the relatively small number of long branches in VLDPE2 compared with LDPEs. In addition, the approximate distributions of short-chain branches of polyethylene blends can be obtained if every component in the blend has the same comonomer and the type of comonomer is known. Therefore, thermal fractionation by DSC is a powerful tool to characterise branched polymers and their blends.

Acknowledgements

One of us (F.C.) would like to acknowledge the RMIT University for providing a Postgraduate Research Scholarship.

References

[1] Wild L. Adv Polym Sci 1991;98:1.
[2] Monrabal B. Crystallisation analysis fractionation (CRYSTAF). J Appl Polym Sci 1994;52:491.
[3] Mara JJ, Menard KP. Acta Polym 1994;45:378.
[4] Zhang M, Huang J, Lynch D, Wanke SE. ANTEC Proc, 1998. p. 539.
[5] Varga J, Menczel J, Solti A. J Therm Anal 1979;17:333.
[6] Kamiya T, Ishikawa N, Kambe S, Ikegami N, Nishibu H, Hattori T. ANTEC Proc, 1990. p. 871.
[7] Adisson E, Ribeiro M, Deffieux A, Fontanille M. Polymer 1992;33:4337.
[8] Balbontin G, Camurati L, Dall'Occo T, Finotti A, Franzese R, Vecellio G. Angew Makromol Chem 1994;219:139.
[9] Balbontin G, Camurati L, Dall'Occo T, Zeigler R. J Mol Catalyst, A: Chem 1995;98:123.
[10] Wolf B, Kenig S, Klopstock J, Miltz J. J Appl Polym Sci 1996;62:1339.
[11] Keating MY, McCord EF. Thermochim Acta 1994;243:129.
[12] Chiu FC, Keating MY, Cheng SZD. ANTEC Proc, 1995. p. 1503.
[13] Keating MY, Lee I-H, Wong CS. Thermochim Acta 1996;284:47.
[14] Fu Q, Chiu F-C, McCreight KW, Guo M, Tseng WW, Cheng SZD, et al. J Macromol Sci, Phys B 1997;36:41.
[15] Starck P. Polym Int 1996;40:111.
[16] Pietikäinen P, Starck P, Seppälä JV. J Polym Sci, Part A: Polym Chem 1999;37:2379.
[17] Starck P, Lehmus P, Seppälä JV. Polym Engng Sci 1999;39:1444.
[18] Karoglanian SA, Harrison IR. Thermochim Acta 1992;212:143.
[19] Müller AJ, Hernández ZH, Arnal ML, Sánchez JJ. Polym Bull 1997;39:465.
[20] Shanks RA, Drummond KM. ANTEC Proc, 1998. p. 2004.
[21] Cser F, Hopewell JL, Shanks RA. J Therm Anal 1998;54:707.
[22] Shanks RA, Amarasinghe G. J Therm Anal Calorimetry 2000;59:471.
[23] Shanks RA, Amarasinghe G. Polymer 2000;41:4579.
[24] Drummond KM, Hopewell JL, Shanks RA. J Appl Polym Sci 2000;78:1009.
[25] Voigt-Martin IG, Alamo R, Mandelkern L. J Polym Sci, Polym Phys Ed 1986;24:1283.
[26] Zhou X, Hay JN. Eur Polym J 1993;29:291.
[27] Hill MJ, Morgan R, Barham PJ. Polymer 1997;38:3003.
[28] Liu W, Kim S, Lopez J, Hsiao B, Keating MY, Lee I-HJ, et al. J Therm Anal Calorimetry 2000;59(4):245.
[29] Arnal ML, Sánchez JJ, Müller AJ. ANTEC Proc, 1999. p. 2329.
[30] Arnal ML, Hernández ZH, Matos M, Sánchez JJ, Méndez G, Sánchez A, et al. ANTEC Proc, 1998. p. 2007.

[31] Arnal ML, Balsamo V, Ronca G, Sánchez A, Müller AJ, Canizales E, et al. J Therm Anal 2000;59:451.
[32] Balsamo V, Müller AJ, Stadler R. Macromolecules 1998;31:7756.
[33] Speed CS. Plast Engng 1982(7):39.
[34] Hill MJ, Barham PJ. Polymer 1997;38:5595.
[35] Schellenberg J, Wagner B. J Therm Anal 1998;52:275.
[36] Zhao Y, Liu S, Yang D. Macromol Chem Phys 1997;198:1427.
[37] Tanem BS, Stori A. Thermochim Acta 2000;345:73.
[38] Lee SY, Jho JY. J Ind Engng Chem 1998;4:170.
[39] Woo L, Westphal SP, Ling TK, Khare AR. Polym Prepr 1998;39:203.
[40] Hosoda S. Polym J 1988;20:383.
[41] Shanks RA. Personal communication.
[42] Müller AJ, Balsamo V, Rosales CM. Polym Network Blends 1992;2:215.
[43] Fonseca CA, Harrison IR. Thermochim Acta 1998;313:37.
[44] Puig CC. Polym Bull 1996;36:361.
[45] Minick J, Moet A, Baer E. Polymer 1995;36:1923.
[46] Joskowicz PL, Muñoz A, Barrera J, Müller AJ. Macromol Chem Phys 1995;196:385.
[47] Galante MJ, Mandelkern L, Alamo RG. Polymer 1998;39:5105.
[48] Butler TL, Lai SY, Patel R. J Plast Film Sheeting 1994;10:102.
[49] Chum PS, Kao CI, Knight GW. Plast Engng 1995(6):21.
[50] Hill MJ, Barham PJ. Polymer 2000;41:1621.
[51] Chen F, Shanks RA, Amarasinghe G. J Appl Polym Sci (In Press).